Structures and Bonding in Silane Derivatives with One Alkali Atom

L. F. Pacios,*,† O. Gálvez,‡ and P. C. Gómez‡

Departamento de Química y Bioquímica, ETSI Montes, Universidad Politécnica de Madrid, E−28040 Madrid, Spain, and Departamento de Química Física I, Facultad de Química, Universidad Complutense de Madrid, E-28040 Madrid, Spain

Received: March 7, 2000; In Final Form: May 17, 2000

The structures of silane derivatives with one alkali atom M, SiX_3M, where X stands for hydrogen or halogen atoms and M is Li or Na, are studied ab initio with uncorrelated and correlated methods and a 6-311++G-(3df,pd) basis set. Geometry, energetics, dipole moments, and topological features of the electron distribution are investigated at the B3LYP/6-311++G(3df,pd) level of the theory for both tetrahedral and inverted structures of these compounds. With the exception of SiH_3Na, the inverted forms have been found to be more stable than the tetrahedral structures. The special geometrical features displayed by these inverted structures are analyzed, paying special attention to the information provided by the electron density. The nature of the bonding in these molecules is finally discussed.

Introduction

It has been known for years that some organic tetracoordinated compounds may present structures distinct to the expected tetrahedral-like geometry. A large number of anomalous examples have been reported in the past twenty years for simple methane and silane derivatives containing halogens and alkali metals (see ref 1 and quotations therein). These geometries resemble an inverted umbrella-like shape with the bond between carbon (or silicon) and the alkali atom as the stick of the umbrella. For methane derivatives, CCl_3Li[1,2] displays this inverted structure as the lowest lying conformer of the minima on its potential energy surface. In the case of one-silicon derivatives, silyl-lithium, SiH_3Li,[1,3] has been more thoroughly studied than any other silanes presenting these anomalous structures. For this molecule, the inverted C_{3v} geometry was found to be more stable than the tetrahedral one by 2.4 kcal mol^{-1} in an ab initio MP4SDTQ/6-31G** calculations at geometries optimized with the 6-31G* basis set.[1] Our recent B3LYP/6-311++G(3df,pd) optimized geometries[3] point to 3.1 kcal mol^{-1} as a probably more accurate estimate of that energy difference.

The interest in elucidating the reasons for which one-carbon or one-silicon compounds may prefer the inverted instead of the conventional tetrahedral geometries is evident. However, theoretical studies on this problem are scarce, whereas experimental data are even less abundant. Apart from the review (already a classic in the literature on Quantum Chemistry) on the ab initio methodology by Hehre, Radom, Schleyer, and Pople,[4] we are aware of only two more recent reports on HF and MP2 calculations with basis sets of double-ζ quality.[5,6] Regarding experimental data, the synthesis of silyl-lithium and silyl-sodium as stable monomers in solution was reported time ago.[7]

Schleyer and Clark[1] pointed out the electrostatic interaction between the SiH_3^- moiety and Li^+ being more favorable in the inverted geometry because of the large negative charge on hydrogens and reported ab initio results confirming this conjecture. We also explored this suggestion in studying the tetrahedral and inverted structures for compounds of stoichiometry $SiF_nH_{3-n}Li$, $n = 0, 3$, finding also a clear stability for inverted geometries rationalizable in terms of electrostatic contributions.[3] In fact, when n increases, the charge on Si increases noticeably and so does the energetic stabilization of the inverted geometry going from 8.1 kcal mol^{-1} when $n = 1$, to 11.7 kcal mol^{-1} for $n = 2$ to 17.4 kcal mol^{-1} for $n = 3$ (B3LYP/6-311++G(3df,-pd) data). However, a surprising result in this study was that $SiBr_3Li$ displays an inverted structure 23.8 kcal mol^{-1} more stable than the tetrahedral one, despite the halogen being now less electronegative than fluorine. Moreover, this molecule displays this extra stability for the inverted form without any clear apparent electrostatic interaction as far as atomic charges and dipole moments are concerned ($SiBr_3Li$ had actually the lowest dipole moment among all the compounds studied). On the other side, silane derivatives with sodium instead of lithium happen to display energetic stabilizations for inverted forms lower than lithium derivatives. However, if one thinks that Na is more electropositive and polarizable than Li, one should expect now more pronounced electrostatic contributions.

We suggested that the covalent character of the interaction between halogens and the alkali atom and between halogens and silicon also play a role in understanding the stability of some inverted structures. The study undertaken in our previous paper[3] with the ab initio calculation of the structures, energetics and properties of $SiX_nH_{3-n}Li$, with X= F, Br, and $SiF_nH_{3-n}Na$, is completed here with $SiCl_3Li$, $SiCl_3Na$, and $SiBr_3Na$. The results presented in this work complete the set of compounds SiX_3M, with X covering the sequence H, F, Cl, and Br and M = Li, Na. In addition, the structural and energetic issues considered before for the first set of silane derivatives is here complemented with special attention payed to the analysis of the electron density. The information gathered after these two complementary studies allows us to present here a whole picture of the nature of bonding in these molecules.

* Corresponding author. E-mail: lpacios@montes.upm.es
† Universidad Politécnica de Madrid.
‡ Universidad Complutense de Madrid.

10.1021/jp0008896 CCC: $19.00
Published on Web 07/19/2000

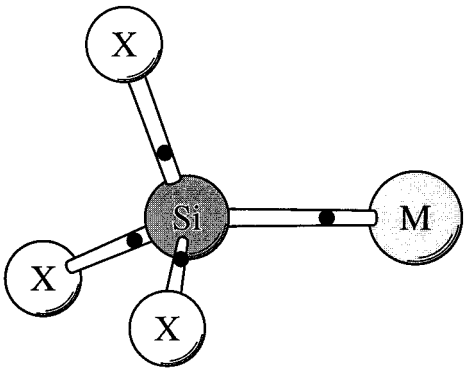

Figure 1. Prototypical tetrahedral structure of SiX_3M silanes, where X stands for H, F, Cl, and Br and the alkali atom M is Li and Na. Bond critical points are indicated by black dots. This figure has been prepared using MolScript.[19]

The paper is organized as follows. In the next section the ab initio methodology employed is briefly presented. The results regarding geometries and energetics are then exposed. Afterward, we focus on the charge distribution by studying atomic charges and dipole moments as well as the information provided by the topological analysis of the electron density ρ. We finally discuss the nature of the bonding in these molecules summarizing the results and presenting our main conclusions.

Methodology

The reliability of density functional theory (DFT) methods for ab initio correlated calculations is currently an issue well established. For the type of molecules considered here, the good performance of Becke's three parameter hybrid functional B3LYP[8] when used with a basis of enough flexibility such as the 6-311++G(3df,pd) set has been previously tested.[3] Our results demonstrated that this choice virtually saturates the basis. We have therefore performed geometry optimizations at the B3LYP/6-311++G(3df,pd) level for both tetrahedral and inverted structures of the silanes with formulas SiX_3M, with X = H, F, Cl, Br and M = Li, Na.

We have also optimized both types of geometries at the HF/6-311++G(3df,pd) and B/6-311++G(3df,pd) levels of theory. While the Hartree−Fock method is the obvious choice for uncorrelated ab initio calculations, our choice for the second method deserves a comment. B stands for DFT Becke's functional for exchange, which includes a nonlocal correction in terms of the gradient of the density to the Slater local exchange.[9] With this method we have intended to complete the test presented in our previous paper about the incidence of correlation effects on the tetrahedral/inverted stability. While we considered then four different correlated methods, only HF was used for the uncorrelated data.

Zero point energy (ZPE) corrections to the energy difference between tetrahedral and inverted geometries have been obtained in ab initio calculations of vibrational frequencies at the B3LYP/6-311++G(2d,p) level of theory. Two population analyses have been performed: the first one is the Merz−Kollman (MK) procedure with the additional constrain to reproduce dipole moments.[10,11] The second is the natural bond orbital (NBO) analysis of the one-electron density matrix.[12,13] Atomic charges as well as dipole moments have been computed with the B3LYP/6-311++G(3df,pd) density. The topological analysis of the density as prescribed by Bader in his theory of atoms in molecules[14] has been done at the B3LYP/6-311++G(2d,p) level. All of the calculations have been performed using the GAUSSIAN 94[15] and GAUSSIAN 98[16] programs.

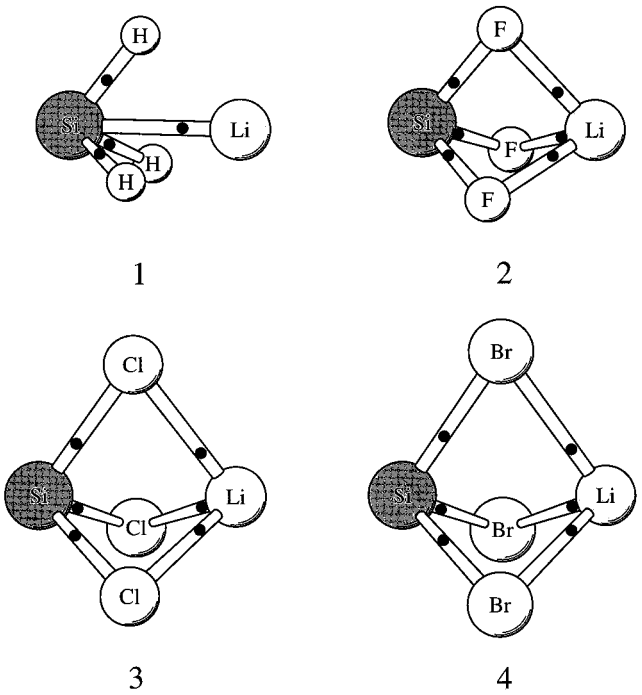

Figure 2. Inverted structures of SiX_3Li silanes, where X stands for H, F, Cl, and Br, optimized in B3LYP/6-311++G(3df,pd) ab initio calculations. Bond critical points determined with the B3LYP electron density are indicated by black dots. This figure has been prepared using MolScript.[19]

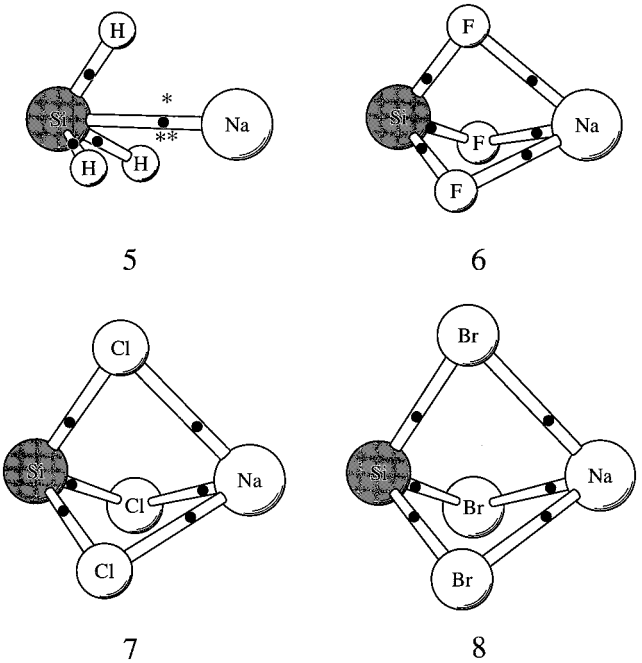

Figure 3. Inverted structures of SiX_3Na silanes, where X stands for H, F, Cl, and Br, optimized in B3LYP/6-311++G(3df,pd) ab initio calculations. Bond critical points determined with the B3LYP electron density are indicated by black dots. Three critical points with special features (see the text) in SiH_3Na are indicated by asterisks. This figure has been prepared using MolScript.[19]

Geometries and Energies

Figure 1 plots the prototypical tetrahedral structure of SiX_3M molecules, while the inverted structures with M = Li are displayed in Figure 2 and M = Na in Figure 3. We have drawn bonds only when critical points of the electron density, indicated by black dots, are found (see the discussion below). Table 1

TABLE 1: B3LYP/6-311++G(3df,pd) Optimized Geometries of Tetrahedral and Inverted Structures of SiX_3M Silanes, X = H, F, Cl, Br; M = Li, Na[a]

parameter[b]	tetrahedral	inverted	parameter[b]	tetrahedral	inverted
	SiH_3Li			SiH_3Na	
SiLi	2.463	2.331	SiNa	2.758	2.706
SiH	1.501	1.575	SiH	1.500	1.558
HLi		1.863	HNa		2.252
HSiLi	115.6	52.77	HSiNa	115.2	56.30
HSiH	102.7	87.18	HSiH	103.2	92.19
	SiF_3Li			SiF_3Na	
SiLi	2.458	2.369	SiNa	2.753	2.741
SiF	1.626	1.741	SiF	1.629	1.729
FLi		1.904	FNa		2.237
FSiLi	115.7	52.52	FSiNa	115.8	54.54
FSiF	102.6	86.82	FSiF	102.4	89.72
	$SiCl_3Li$			$SiCl_3Na$	
SiLi	2.451	2.667	SiNa	2.752	3.089
SiCl	2.118	2.266	SiCl	2.123	2.261
ClLi		2.335	ClNa		2.673
ClSiLi	115.0	55.79	ClSiNa	115.2	57.48
ClSiCl	103.5	91.47	ClSiCl	103.2	93.81
	$SiBr_3Li$			$SiBr_3Na$	
SiLi	2.451	2.765	SiNa	2.754	3.190
SiBr	2.300	2.452	SiBr	2.308	2.448
BrLi		2.495	BrNa		2.830
BrSiLi	114.3	56.78	BrSiNa	114.6	58.49
BrSiBr	104.2	92.85	BrSiBr	103.8	95.18

[a] In all structures, the dihedral angle XSiMX is ±120 degrees. [b] Bond distances are in Å, bond angles in degrees.

collects the geometrical parameters whose main features may be remarked as follows.

The Si−M bond lengths are essentially constant in tetrahedral geometries while they increase noticeably with the size of the halogen in the inverted structures. If one considers the commonly accepted covalent radii[17] (Li = 1.23 Å, Na = 1.57 Å, Si = 1.17 Å), Si−Li and Si−Na covalent bonds should display distances about 2.40 and 2.74 Å, respectively. It is interesting to note that only when X = H and F (structures 1, 2, 5, and 6), Si−M bond lengths are below these values, while the other inverted structures exhibit longer distances. For inverted geometries with Cl and Br (structures 3, 4, 7, and 8), Si−Li and Si−Na bond lengths are so large that one is tempted to discard a covalent bond without any further consideration. On the other side, Si−X distances are consistently maintained regardless of the alkali atom and only with X = Br their values are slightly larger than the covalent lengths expected from the atomic radii.[17] Although X−M distances are redundant parameters, we include them in Table 1 because, as the analysis of ρ suggests, the halogens and the alkali M in inverted geometries are actually bonded (see Figures 2 and 3).

For all of the tetrahedral geometries, bond angles happen to lie in a narrow range: XSiM angles between 114.3° in BrSiNa and 115.8° in FSiNa and XSiX angles between 102.4° in FSiF and 104.2° in BrSiBr. These values are consistent with the distortion from the regular tetrahedral produced by the larger distance between Si and M. For inverted structures, XSiM angles vary slightly from 53° when X = H to 58° for X = Br. These inverted geometries may better be viewed as triangular bipyramidal structures with an equatorial plane defined by the group X_3 and an axis defined by the Si−M bond. From geometries in Table 1 it is easy to determine that this plane intersects the Si−M line at a distance about 0.41−0.49 times the Si−M length for lithium derivatives and about 0.32−0.40 for sodium compounds, in both cases closer to the silicon atom.

The uncorrelated HF/6-311++G(3df,pd) and B/6-311++G(3df,pd) geometries (data not shown) display the same overall picture, although the lack of correlation yields longer bond distances, especially notorious for the Si−M bond. Concerning bond angles, these uncorrelated results are in close agreement with B3LYP values, being again HF and B angles slightly larger than the correlated ones.

Table 2 lists total energies for the optimized geometries while the relative stability between them is summarized in Table 3. The HF calculations overestimate the stability of tetrahedral structures in hydrogenated silanes. Even in SiH_3Na, where all of the theoretical evidence points to the tetrahedral geometry as the preferred structure, the HF relative stability is about twice the value predicted by the other methods. For SiH_3Li, only the HF results predict the tetrahedron as the favored geometry. Halogenated silanes are invariably more stable in the inverted

TABLE 2: Total Minimum Energies (E_h) for Tetrahedral and Inverted Structures of SiX_3M Silanes, X = H, F, Cl, Br; M = Li, Na, Obtained in Ab Initio Calculations with the 6-311++G(3df,pd) Basis Set at Three Levels of Theory[a]

		tetrahedral			inverted		
molecule	relative to	HF	B	B3LYP	HF	B	B3LYP
SiH_3Li	−298	−0.112440	−0.087280	−0.832971	−0.108197	−0.090835	−0.837766
SiF_3Li	−595	−0.027888	−0.175054	−1.896543	−0.045650	−0.201367	−1.924046
$SiCl_3Li$	−1675	−0.100532	−0.051264	−2.902744	−0.126082	−0.087740	−2.938045
$SiBr_3Li$	−8013	−0.679233	−0.877185	−6.655004	−0.708440	−0.915934	−6.692849
SiH_3Na	−452	−0.511933	−0.515266	−1.613772	−0.503267	−0.510797	−1.609879
SiF_3Na	−749	−0.427057	−0.602304	−2.676429	−0.441371	−0.618036	−2.694281
$SiCl_3Na$	−1829	−0.502165	−0.479908	−3.684162	−0.524290	−0.507000	−3.710334
$SiBr_3Na$	−8168	−0.082136	−0.306528	−6.437078	−0.108365	−0.336941	−6.466768

[a] Uncorrelated Hartree−Fock (HF) and Becke's functional for exchange only (B) and correlated hybrid Beckes's three parameter functional (B3LYP).

TABLE 3: Energy Differences ΔE[a] between Tetrahedral and Inverted Structures of SiX_3M Silanes, X = H, F, Cl, Br; M = Li, Na, Obtained with the 6-311++G(3df,pd) Basis Set at the Hartree−Fock (HF), DFT Becke's Exchange (B), and Hybrid Functional B3LYP Levels of Theory

molecule	HF[b]	B[b]	B3LYP[b]	B3LYP[c]	molecule	HF[b]	B[b]	B3LYP[b]	B3LYP[c]
SiH_3Li	−2.66	2.23	3.01	3.07	SiH_3Na	−5.44	−2.80	−2.44	−2.00
SiF_3Li	11.2	16.5	17.3	17.4	SiF_3Na	8.98	9.87	11.2	11.5
$SiCl_3Li$	16.0	22.9	22.2	22.0	$SiCl_3Na$	13.9	17.0	16.4	16.5
$SiBr_3Li$	18.3	24.3	23.8	23.6	$SiBr_3Na$	16.5	19.1	18.6	18.7

[a] $\Delta E = E$(tetrahedral) − E(inverted) in kcal mol^{-1}. Positive values mean inverted structures are more stable than tetrahedral geometries. [b] No zero point energy (ZPE) correction included. [c] ZPE corrected values. ZPE corrections were done at the B3LYP/6-311++G(2d,p) level in all cases.

TABLE 4: B3LYP/6-311++G(3df,pd) Atomic Charges[a] and Dipole Moments (μ) of Tetrahedral and Inverted Structures of SiX_3M Silanes, X = H, F, Cl, Br; M = Li, Na

	tetrahedral				inverted			
SiX_3M	Si	X	M	μ[b]	Si	X	M	μ[b]
SiH_3Li	−0.359	−0.065	+0.554	7.169	−0.082	−0.238	+0.796	5.640
SiF_3Li	−0.242	−0.141	+0.665	9.294	+0.243	−0.368	+0.861	4.185
$SiCl_3Li$	−0.541	−0.067	+0.742	9.598	+0.245	−0.303	+0.664	2.945
$SiBr_3Li$	−0.851	+0.007	+0.830	9.672	+0.240	−0.278	+0.594	3.015
SiH_3Na	−0.160	−0.106	+0.478	7.292	−0.084	−0.232	+0.780	7.247
SiF_3Na	−0.097	−0.175	+0.622	10.03	+0.221	−0.389	+0.946	6.833
$SiCl_3Na$	−0.425	−0.096	+0.713	10.67	+0.243	−0.338	+0.771	5.512
$SiBr_3Na$	−0.654	−0.041	+0.777	10.86	+0.223	−0.306	+0.695	5.003

[a] Calculated according to the Merz−Kollman scheme with the constrain to reproduce the computed dipole moment [b] Dipole moments are in debyes

TABLE 5: NBO Atomic Charges Computed with the B3LYP/6-311++G(3df,pd) Electron Density of Tetrahedral and Inverted Structures of SiX_3M Silanes, X = H, F, Cl, Br; M = Li, Na

	tetrahedral			inverted		
SiX_3M	Si	X	M	Si	X	M
SiH_3Li	−0.243	−0.164	+0.735	+0.053	−0.312	+0.883
SiF_3Li	+1.396	−0.691	+0.677	+1.307	−0.756	+0.961
$SiCl_3Li$	+0.451	−0.422	+0.815	+0.762	−0.547	+0.879
$SiBr_3Li$	+0.192	−0.348	+0.852	+0.592	−0.483	+0.857
SiH_3Na	−0.123	−0.173	+0.642	−0.002	−0.278	+0.836
SiF_3Na	+1.453	−0.694	+0.629	+1.296	−0.755	+0.969
$SiCl_3Na$	+0.531	−0.433	+0.768	+0.757	−0.557	+0.914
$SiBr_3Na$	+0.277	−0.361	+0.806	+0.591	−0.497	+0.900

form at all levels of theory, being that the uncorrelated B results in better agreement with B3LYP than with HF results. On the other side, except for SiH_3Na (the most peculiar molecule of the set, as discussed below), the zero point corrections represent almost negligible contributions to the stabilization energy. A firm conclusion arising not only from Tables 2 and 3 but also from the existing evidence[1,3] is that the presence of an halogen does in fact stabilize the inverted geometry.

Energy differences in Table 3 provide interesting information about the suggested electrostatic stabilization in these molecules. Being that fluorine is the most electronegative atom, one should expect larger electrostatic factors in SiF_3M compouds, as it is in fact the case with regard to charge effects (see below). However, the stability of inverted structures increases noticeably when Cl substitutes F and still increases about 2 kcal mol^{-1} when Br replaces Cl. Regarding the alkali atom, since Na is a bit more electropositive than Li, slightly larger electrostatic effects should be expected in the SiX_3Na with respect to SiX_3-Li. As the analysis presented in the next section demonstrates, this happens to be the case concerning charge distributions, but, nevertheless, the inverted structures with sodium display lower energy stabilizations than those containing lithium. To the light of the geometries displayed and these energies, it is evident that the structures shown in Figures 2 and 3 become more stable as the halogen is more voluminous and therefore Si and M atoms are farther apart.

Charge Distributions

Table 4 lists MK atomic charges obtained with the B3LYP/6-311++G(3df,pd) electron density and the additional constraint to reproduce the computed dipole moments, μ, also shown in the table. NBO atomic charges are given in Table 5. Due to the symmetry in all of the structures, the only nonzero dipole component is along the Si−M direction. As expected from the geometry itself, the tetrahedral structures display larger dipoles than the inverted ones. Both hydrogenated tetrahedral silanes exhibit almost identical dipole moments, while the values for the inverted compounds are quite different: a possible explanation of this fact has to be deferred to the discussion on SiH_3Na presented below. Dipole moments for halogenated tetrahedral silanes are about 9.5 D for lithium derivatives and about 10.5 D for sodium derivatives, while the inverted structures display dipoles about half these values. Besides, while μ increases slightly with the size of X in tetrahedral structures, it decreases markedly in the inverted ones.

It is interesting to compare the picture provided by the MK atomic charges which reproduce the dipole moments with the NBO charges obtained from the density matrix. For tetrahedral geometries, the MK charges on hydrogen and halogen atoms are small and negative (with the negligible exception of Br in $SiBr_3Li$). Silicon in these structures has a significant amount of negative charge that increases with the size of the halogen for both alkali derivatives. The alkali atom M displays large positive charges that consistently increase along the sequence X = H, F, Cl, Br. The main factor in polarizing these structures seems to be the presence of M, directly bonded to Si which is assigned a negative charge by the MK analysis. The presence of a negative silicon diminishes then the electronegative role of halogens. Only the special electronegativity of F forces a partial sharing of negative charge with Si in both SiF_3M compounds. In the brominated silanes, the charge on Br is essentially zero and the dipole moment is entirely due to the polarity of the Si−M bond as if it were isolated. The picture provided by the NBO analysis for tetrahedral structures shows marked differences in the SiX_3 moiety, although the charges on M are in reasonable agreeement with MK values. In fact, while the global negative charge of the SiX_3 group is essentially assigned to silicon in the MK analysis, NBO negative charges are assigned to halogens, being shared with Si only in SiH_3M.

The role played by Si and X atoms in the inverted structures from the MK point of view is completely different. While Si has a negative charge about −0.080 in both silanes with hydrogen, it displays a positive charge about +0.240 in the rest of the derivatives. As expected, halogens display negative charges with slightly larger values in the molecules with sodium. In all cases, M is obviously the more positive atom in the molecule with an especially large charge in the presence of fluorines. To understand these charges it is helpful to look at the structures plotted in Figures 2 and 3. For both SiH_3M molecules, the inversion of the three hydrogens around silicon forces the allocation of charge negative on H since they are now closer to the alkali (structures 1 and 5). The negative charge on Si is then decreased and the polarity is essentially due to the interaction between $(H_3)^-$ and Li^+, although a Si−M bond still exists. On the contrary, if X is an halogen the geometry is

TABLE 6: Properties of ρ at (3, −1) Bond Critical Points for Tetrahedral Structures of SiX_3M Silanes, X = H, F, Cl, Br; M = Li, Na, Obtained with the B3LYP/6-311++G(2d,p) Electron Density at the Geometries Given in Table 1

molecule	bond Si−A	r_{bcp}(Si)[a]	r_{bcp}(A)[b]	r(Si-A)[c]	ρ_{bcp}[d]	$\nabla^2\rho_{bcp}$[e]	ϵ[f]
SiH_3Li	Si−Li	1.691	0.772	2.463	0.0295	0.0779	0.0
	Si−H	0.739	0.762	1.501	0.1134	0.1217	0.0636
SiF_3Li	Si−Li	1.692	0.765	2.457	0.0307	0.0844	0.0
	Si−F	0.680	0.946	1.626	0.1294	0.8458	0.0229
$SiCl_3Li$	Si−Li	1.683	0.768	2.451	0.0297	0.0846	0.0
	Si−Cl	0.785	1.333	2.118	0.0895	0.0736	0.0787
$SiBr_3Li$	Si−Li	1.680	0.771	2.451	0.0292	0.0813	0.0
	Si−Br	0.857	1.443	2.300	0.0787	−0.0311	0.0897
SiH_3Na	Si−Na	1.682	1.076	2.758	0.0246	0.0622	0.0
	Si−H	0.738	0.762	1.500	0.1140	0.1194	0.0664
SiF_3Na	Si−Na	1.690	1.062	2.752	0.0255	0.0713	0.0
	Si−F	0.681	0.947	1.628	0.1287	0.8340	0.0248
$SiCl_3Na$	Si−Na	1.686	1.066	2.752	0.0245	0.0706	0.0
	Si−Cl	0.789	1.335	2.124	0.0888	0.0665	0.0826
$SiBr_3Na$	Si−Na	1.683	1.071	2.754	0.0239	0.0680	0.0
	Si−Br	0.866	1.442	2.308	0.0779	−0.0351	0.0896

[a] Distance from bond critical point to silicon. [b] Distance from bond critical point to atom A. [c] Si−A bond length. [d] Electron density at the bond critical point. [e] Laplacian of the electron density at the critical point. [f] Ellipticity of the bond. Distances in Å. ρ_{bcp} and $\nabla^2\rho_{bcp}$ in atomic units.

TABLE 7: Properties of ρ at (3, −1) Bond Critical Points for Inverted Structures of SiX_3M Silanes, X = H, F, Cl, Br; M = Li, Na, Obtained with the B3LYP/6-311++G(2d,p) Electron Density at the Geometries Given in Table 1 and Displayed in Figures 2 and 3

molecule	bond A−B	r_{bcp}(A)[a]	r_{bcp}(B)[b]	r(A−B)[c]	ρ_{bcp}[d]	$\nabla^2\rho_{bcp}$[e]	ϵ[f]
SiH_3Li	Si−Li	1.538	0.793	2.331	0.0250	0.1115	0.0
	Si−H	0.771	0.804	1.575	0.0958	0.0800	0.1140
SiF_3Li	Si−F	0.725	1.016	1.741	0.0979	0.4704	0.0620
	Li−F	0.729	1.175	1.904	0.0288	0.2150	0.1168
$SiCl_3Li$	Si−Cl	0.873	1.393	2.266	0.0710	−0.0065	0.0830
	Li−Cl	0.783	1.552	2.335	0.0215	0.1135	0.1124
$SiBr_3Li$	Si−Br	0.986	1.466	2.452	0.0631	−0.0250	0.0614
	Li−Br	0.806	1.689	2.495	0.0189	0.0875	0.1154
SiH_3Na	Si−Na	1.588	1.118	2.706	0.0188	0.0698	0.0
	Si−H	0.765	0.793	1.558	0.0997	0.0757	0.0929
	H−Na	1.261	0.991	2.252	0.0188	0.0698	6.689
SiF_3Na	Si−F	0.721	1.008	1.729	0.1003	0.4987	0.0533
	Na−F	1.024	1.213	2.237	0.0234	0.1531	0.0994
$SiCl_3Na$	Si−Cl	0.871	1.390	2.261	0.0714	−0.0071	0.0730
	Na−Cl	1.090	1.583	2.673	0.0169	0.0858	0.1048
$SiBr_3Na$	Si−Br	0.985	1.463	2.448	0.0633	−0.0256	0.0481
	Na−Br	1.114	1.716	2.830	0.0152	0.0684	0.0983

[a] Distance from bond critical point to atom A. [b] Distance from bond critical point to atom B. [c] A−B bond length. [d] Electron density at the bond critical point. [e] Laplacian of the electron density at the critical point. [f] Ellipticity of the bond. Distances in Å. ρ_{bcp} and $\nabla^2\rho_{bcp}$ in atomic units.

better seen as a triangular bipyramid with the equatorial plane X_3 (structures 2−4 and 6−8) forming now a negatively charged triangle and a perpendicular axis with positive charges at both ends. Since fluorine is more electronegative, the larger negative F_3 triangle interacts with a more positive alkali atom (charges +0.86 for Li and +0.95 for Na).

The qualitative description of the inverted structures provided by NBO charges in Table 5 is analogous to that of the tetrahedral silanes discussed before, although the values are now larger overall. If one considers the different geometry of both types of structure, as well as their relative stabilities, one should expect also a different picture between them regarding atomic charges. As it is unfortunately common when using population analyses, the results are not of great help in shedding light on the charge distribution in a molecule. However, the analysis of the electron density itself usually allows to gain valuable insight into the nature of a molecule. To perform this task, we have considered the topological information provided by the theory of atoms in molecules.[14]

Table 6 summarizes the bond critical points (bcp) of the electron density ρ, r_{bcp}, in the tetrahedral structures, and Table 7 gives them for the inverted structures. We list the location of r_{bcp}, the values at this point of the density, ρ_{bcp} and its laplacian, $\nabla^2\rho_{bcp}$, respectively, and the ellipticity of the bond, ϵ. The bcp for the inverted geometries are indicated by black dots in Figures 2 and 3, where we have drawn bonds only when a critical point in the corresponding bond path has been found. All of the critical points collected in Tables 6 and 7 are saddle points at which two curvatures (λ_1 and λ_2) of the density are negative and one is positive, i.e., (3, −1) points. For bonded atoms, the electron density attains its minimum along the bond line at r_{bcp} and reaches its maximum at r_{bcp} in the plane perpendicular to the bond path defined by the axes of curvature of λ_1 and λ_2. If λ_2 is the smallest value, then the ellipticity of the bond is defined as $\epsilon = (\lambda_1/\lambda_2 - 1)$, and it gives a measure of the extent to which ρ is accumulated in a plane containing the bond path. If a bond has cylindrical symmetry, $\lambda_1 = \lambda_2$ and $\epsilon = 0.0$. If some density is accumulated in a perpendicular plane containing the bond, then ϵ illustrates the amount of this accumulation. As an illustrative example, the ellipticities of the C−C bond in ethane, benzene, and ethylene are 0.0, 0.23, and 0.45, respectively.[14] On the other hand, the decrease in the value of λ_2 and its eventual disappearance is intepreted as a sign of an unstable bond whose rupture allows to gain stability. A structure with a bond displaying an unusually large ellipticity is thus potentially unstable. For example, $\epsilon = 6.7$ is found in a bond of the cyclopropylcarbinyl cation, $C_4H_7^+$, which breaks to an open structure much more stable.[18] The laplacian of the density $\nabla^2\rho(\mathbf{r})$ is useful to characterize how the charge density is distributed: in regions where $\nabla^2\rho < 0$, the charge is locally concentrated, while $\nabla^2\rho > 0$ indicates local depletion of charge.

The bcp in Tables 6 and 7 share common features. Density values at the minimum are typically below 0.1 au, with the only exception being Si−H and Si−F bonds in the tetrahedral structures, where they increase to 0.11 and 0.13 au, respectively. The magnitude of $\nabla^2\rho_{bcp}$ is very low and positive, except for the Si−Br bond in both geometries where it is about −0.03 au. The picture provided by these low values at the (3, −1) critical points is known to be characteristic of atomic interactions of the closed-shell type (in Bader's terminology), such as ionic bonds, noble gas repulsive states, hydrogen bonds or van der Waals systems.[14] With the exception of H−Na bonds in SiH_3-Na, treated below, the ellipticities present also very low values, a feature indicative of essentially cylindrical symmetry. The negligible accumulation of charge in planes perpendicular to the bonds suggests therefore that the electron distributions are typical of single bonds. Concerning the location of bcp, data in Table 6 reveal that they lie at a distance about 1.69 Å from Si in the Si−M bonds in tetrahedral structures while this distance obviously increases with the size of the halogen in Si−X bonds without any apparent dependence on the alkali. For the inverted structures, the position of the bcp as summarized in Table 7 and depicted in Figures 2 and 3 is now closer to silicon in Si−X bonds at a location about 0.40 times the bond length. For X−M bonds the critical point is closer to M in these inverted geometries.

Hydrogenated inverted structures 1 and 5 deserve particular comment. Only in them is a bond in the sense of the theory of

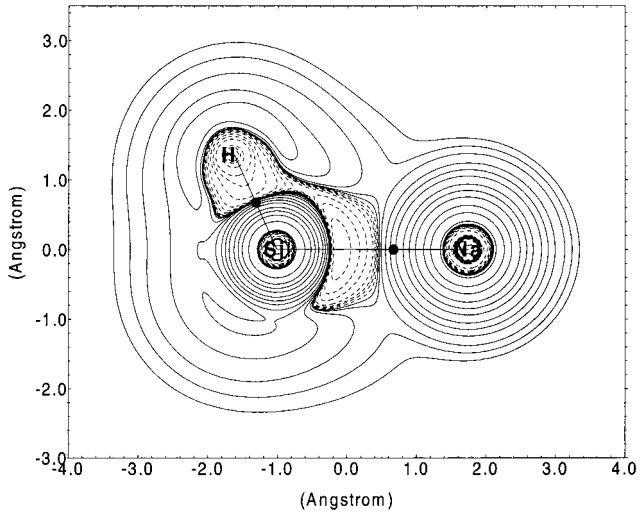

Figure 4. Contour map of the laplacian of the B3LYP electron density in the plane defined by H, Si, and Na atoms in the optimized B3LYP/6-311++G(3df,pd) tetrahedral geometry of SiH_3Na. Bond critical points are indicated by black dots. Positive values of $\nabla^2\rho$ are denoted by solid contours, negative values by dashed contours. The outermost contour equals +0.002 au, and the remaining contours increase and decrease from a zero contour in steps $\pm 2 \times 10^n$, $\pm 4 \times 10^n$, $\pm 8 \times 10^n$, with $n = -3, -2, -1, 0, 1$, and 2.

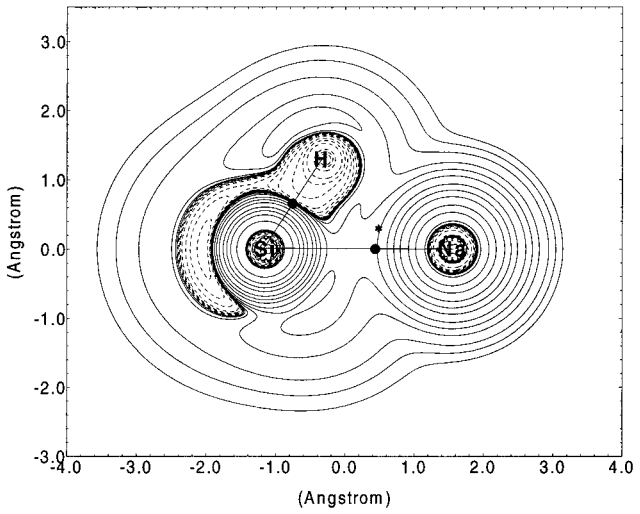

Figure 5. Contour map of the laplacian of the B3LYP electron density in the plane defined by H, Si, and Na atoms in the optimized B3LYP/6-311++G(3df,pd) inverted geometry of SiH_3Na, structure 5. Bond critical points are indicated by black dots. The asterisk indicates a critical point with special features (see the text). See Figure 4 for contour values.

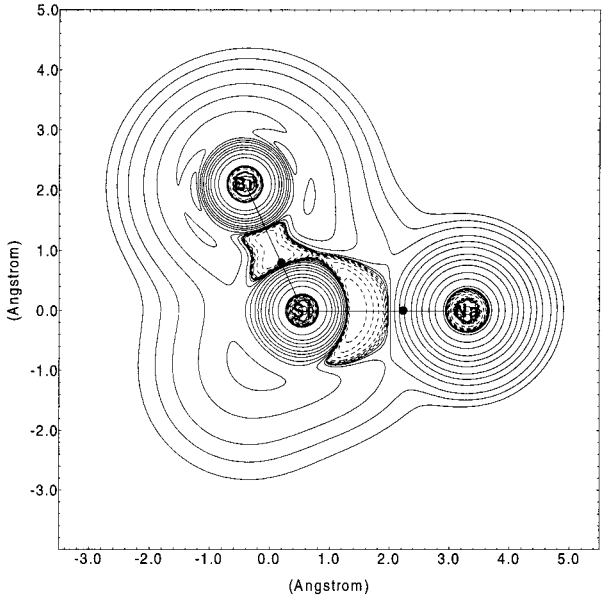

Figure 6. Contour map of the laplacian of the B3LYP electron density in the plane defined by Br, Si, and Na atoms in the optimized B3LYP/6-311++G(3df,pd) tetrahedral geometry of $SiBr_3Na$. Bond critical points are indicated by black dots. See Figure 4 for contour values.

atoms in molecules identified between Si and M, while no bond exists between H and M. The sodium derivative, structure 5, is unique in exhibiting a third type of critical point in H−Na bond paths with an anomalous $\epsilon = 6.69$. As commented above, such a high ellipticity is indicative of unstable bonds. The position of these three critical points is indicated in Figure 3 by asteriks which lie on a curved path joining sodium and the three hydrogens (not drawn). This anomalous ϵ suggests the rupture of possible H−Na bonds, precluding thus the formation of the X−M links that lead to the bipyramidal structures displayed by halogenated silanes. It is remarkable that SiH_3Na is the only compound for which the tetrahedral geometry is predicted to be more stable to all levels of theory considered, while the correlated results for SiH_3Li agree qualitatively with the rest of silanes.

To end this section, we plot contour maps of $\nabla^2\rho$ for the tetrahedral and inverted geometries of SiH_3Na in Figures 4 and 5, respectively. Figures 6 and 7 display the same maps for $SiBr_3Na$. In both molecules, we have selected the XSiNa plane in order to compare the distinctive features of the local concentration or depletion of charge. The particular values of these contours are not as important as the relative location of the regions where the laplacian undergoes a change in sign. The inner contours around each nucleus correspond to the spike-like concentrations of ρ on it. Interatomic regions of negative $\nabla^2\rho$ encompass the sharing of electronic charge indicative of covalently bonded atoms. In shared interactions, the regions with $\nabla^2\rho < 0$ contain the bcp and they are contiguous over the valence regions of atoms. On the other side, closed-shell interactions, such as those found in ionic bonds or hydrogen bonds, are dominated by the contraction of charge away from interatomic regions where consequently $\nabla^2\rho > 0$.

A common feature in all of these maps is that the shared negative region of the laplacian around atoms found in common covalent bonds is absent. However, in both hydrogenated silanes there is a region of charge concentration which extends covering H atoms and partly encircles Si. This reveals the presence of a belt of charge concentration around Si pointing toward Na in the tetrahedron (Figure 4) and pointing to the opposite direction in the inverted structure (Figure 5). The Si−H bond is thus partially favored in a convalent sense by these belts of charge, especially in SiH_3Na where it also includes hydrogens. In the brominated silanes, a $\nabla^2\rho < 0$ region again appears around Si with the same relative orientation with respect to sodium, including now the bcp but not the Br atom (Figures 6 and 7). As a consequence, these Si−Br bonds may be regarded as less covalent than the equivalent Si−H links. Concerning Si−Na bonds, two qualitatively different situations arise. In the tetrahedral structure the $\nabla^2\rho < 0$ region around Si extends also to cover part of the Si−Na bond. Thus, although no real shared interaction is revealed, there is a region where charge is partially concentrated between atoms. On the contrary, the interatomic region between Si and Na in the inverted geometries (Figures 5 and 7) is dominated by the $\nabla^2\rho > 0$ behavior indicative of charge depletion. Since the belt of charge concentration around Si points toward the direction opposite to sodium, a covalent

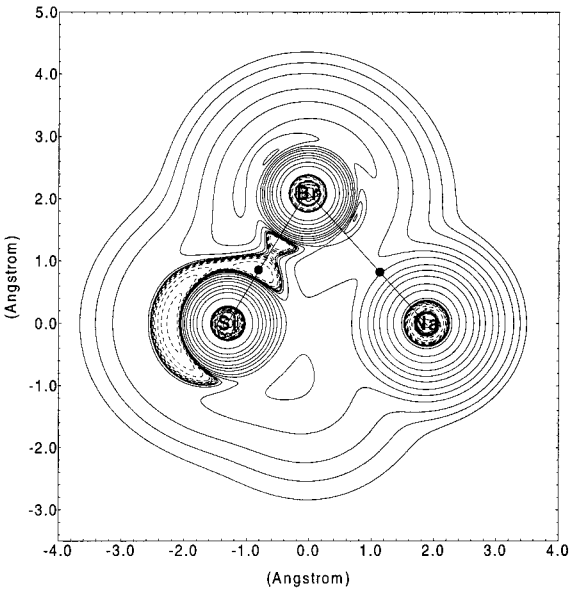

Figure 7. Contour map of the laplacian of the B3LYP electron density in the plane defined by Br, Si, and Na atoms in the optimized B3LYP/6-311++G(3df,pd) inverted geometry of $SiBr_3Na$, structure 8. Bond critical points are indicated by black dots. See Figure 4 for contour values.

Si−Na bond is clearly precluded in these geometries. Finally, the circular $\nabla^2\rho > 0$ contours around all of the atoms except H are indicative of contractions in ρ toward each of the nuclei, a feature identified in predominantly ionic molecules such as NaF or LiCl.[14] Maps for silanes with lithium instead sodium (not shown) exhibit exactly the same features except for the obviously smaller size of the $\nabla^2\rho > 0$ regions around Li.

Discussion

One-silicon derivatives containing one alkali atom M, SiX_3M, present inverted structures progressively more stable in the sequence X = H, F, Cl, and Br with respect to tetrahedral geometries. This result is supported by ab initio calculations performed with the 6-311++G(3df,pd) basis set, flexible enough so as to be considered virtually saturated. Electron correlation effects seem to affect especially SiH_3Li, the only case for which uncorrelated and correlated results do not agree. Besides, SiH_3Na is the only molecule predicted to be slightly more stable in tetrahedral geometry in both correlated and uncorrelated calculations. When X is an halogen, our data clearly indicate an increase in the stability of inverted versus tetrahedral structures, especially notorious when X changes from F to Cl and a little further in going from Cl to Br. This result is supported by methods so disparate as HF, B, or B3LYP and our previous studies in similar compounds.[3] Concerning the alkali atom, we have found the inverted silanes containing Li comparatively more stable than the analogous compounds with Na.

The inverted geometries for halogenated silanes resemble triangular bipyramidal structures with the group X_3 forming the equatorial triangular plane and Si and M atoms defining the perpendicular axis. In these structures, the halogen X happens to display a kind of bridged bond between Si and M, while no real bond between these two atoms is identified. This picture is supported not only by the geometrical parameters but also by the topological analysis of the electron density provided by the theory of atoms in molecules. In fact, for the halogenated inverted silanes, critical points in bond paths between Si and X on one hand and between X and M on the other hand are found, but not on the path between Si and M.

Only SiH_3M displays geometries that may be viewed as genuine inverted structures, and only in them are critical points identified between Si and M and not between X = H and M. SiH_3Na is a special case in that it exhibits critical points between sodium and the three hydrogens indicative of an unstability associated to a type of link that it is otherwise present in halogenated derivatives, namely the X−Na bond.

The information provided by the critical points and the laplacian of ρ suggests a type of bonding dominated by closed-shell-like interactions indicative of predominantly ionic bonds. There is little sharing of electron density betwen atoms in all of the structures, and only for Si−H bonds in the hydrogenated silanes has a region of charge shared by atoms and bonds been found. For the halogenated derivatives only when the halogen is bromine, the laplacian indicates the presence of charge concentration in bond regions reminiscent of usual covalent environments. The whole picture is clearly supported by the atomic charges and dipole moments that reveal a strong ionic character in all of the structures, with the possible exception of inverted $SiCl_3Li$ and $SiBr_3Li$. For tetrahedral geometries, the Si−M bond is essentially the bond responsible for this interaction with large positive charges on M and large negative charges on Si and with the X_3 group playing a secondary role in this regard. For inverted structures, on the contrary, the axis Si−M has positive charges at both ends while the X_3 group forms now a ring of negative charges.

From the results and analyses presented in this work we finally suggest the following schematic picture of the bonding in these SiX_3M silanes. The alkali atom M is the primary factor for polarizing the molecules. If M is directly linked to silicon as it is the case in tetrahedral geometries, the ionic interaction between the $(SiX_3)^-$ moiety and M^+ is essentially linked to the Si−M bond. Due to the marked electronegativity of halogens as compared to hydrogen, it seems reasonable to consider more favorable the bond between a negative silicon and hydrogen than the bond with an halogen. This could account for the stability of tetrahedral geometries in SiH_3M molecules.

On the contrary, for the inverted geometries the polarization produced by the alkali atom affects primarily X atoms that consequently display noticeable negative charges. If X is a halogen, the whole interaction is then obviously favored, which might explain the stability of these geometries for the halogenated silanes. However, the interesting finding in this case is that the structure is arranged in the form of a triangular bipyramidal geometry instead of a kind of inverted tetrahedron. The ionic interaction should be now produced by the triangle $(X_3)^-$ and the perpendicular axis defined by Si^+ and M^+. Since now the halogen acts as a bridge between silicon and the alkali atom, the more voluminous bromine should favor this structure, which is consistent with the slight covalent character found precisely in $SiBr_3M$.

Finally, to understand the larger stability in lithium-inverted structures with respect to the analogous sodium structures is a bit more complicated. We can risk the following explanation. Since lithium is much smaller than sodium, the shorter distances involved in ionic effects with Li should allow slightly more stable overall interactions than those corresponding to Na. This conjecture is supported by our data: while the interatomic distances in silanes with lithium are notoriously shorter than those of sodium derivatives, the positive atomic charges on sodium are not much more larger than those of lithium. In fact, if one estimates the ionic energy associated with atomic charges and distances in both structures, molecules with lithium happen

to yield energies noticeably lower in a magnitude about 10% for X = F and about 5% for X = Cl and Br.

Acknowledgment. The authors gratefully acknowledge financial support from the Dirección General de Enseñanza Superior e Investigación Científica, Project No PB97-0268.

References and Notes

(1) Schleyer, P. v. R.; Clark, T. *J. Chem. Soc., Chem. Commun.* **1986**, 1371.
(2) Clark, T.; Schleyer, P. v. R. *J. Am. Chem. Soc.* **1979**, *101*, 7747.
(3) Gómez, P. C.; Alcolea Palafox, M.; Pacios, L. F. *J. Phys. Chem. A* **1999**, *103*, 8357.
(4) Hehre, W. J.; Radom, L.; Schleyer, P. v. R.; Pople, J. A. *Ab Initio Molecular Orbital Theory*; John Wiley & Sons: New York, 1986.
(5) Zyubin, A. S.; Zyubina, T. S.; Charkin, O. P. *Russ. J. Inorg. Chem.* **1991**, *36*, 188.
(6) Alcolea Palafox, M. *Asian J. Phys.* **1995**, *4*, 169.
(7) Morrison, J. A.; Ring, M. A. *Inorg. Chem.* **1967**, *6*, 100.
(8) Becke, A. D. *J. Chem. Phys.* **1993**, *98*, 5648.
(9) Becke, A. D. *Phys. Rev. A* **1988**, *38*, 3098.
(10) Singh, U. C.; Kollman, P. A. *J. Comput.Chem.* **1984**, *5*, 129.
(11) Besler, B. H.; Merz, K. M., Jr.; Kollman, P. A. *J. Comput. Chem.* **1990**, *11*, 431.
(12) Reed, A. E.; Weinstock, R. B.; Weinhold, F. *J. Chem. Phys.* **1985**, *83*, 735.
(13) Reed, A. E.; Weinhold, F.; Curtiss, L. A. *Chem. Rev.* **1988**, *88*, 899.
(14) Bader, R. F. W. *Atoms in Molecules. A Quantum Theory*; Oxford University Press: Oxford, U.K., 1990.
(15) Frisch, M. J.; Trucks, G. W.; Schlegel, H. B.; Gill, P. M. W.; Johnson, B. G.; Robb, M. A.; Cheeseman, J. R.; Keith, T.; Petersson, G. A.; Montgomery, J. A.; Raghavachari, K.; Al-Laham, M. A.; Zakrzewski, V. G.; Ortiz, J. V.; Foresman, J. B.; Cioslowski, J.; Stefanov, B. B.; Nanayakkara, A.; Challacombe, M.; Peng, C. Y.; Ayala, P. Y.; Chen, W.; Wong, M. W.; Andres, J. L.; Replogle, E. S.; Gomperts, R.; Martin, R. L.; Fox, D. J.; Binkley, J. S.; Defrees, D. J.; Baker, J.; Stewart, J. P.; Head-Gordon, M.; Gonzalez, C.; Pople, J. A. *GAUSSIAN 94 Rev. C.2*; Gaussian Inc.: Pittsburgh, PA, 1995.
(16) Frisch, M. J.; Trucks, G. W.; Schlegel, H. B.; Scuseria, G. E.; Robb, M. A.; Cheeseman, J. R.; Zakrzewski, V. G.; Montgomery, J. A., Jr.; Stratmann, R. E.; Burant, J. C.; Dapprich, S.; Millam, J. M.; Daniels, A. D.; Kudin, K. N.; Strain, M. C.; Farkas, O.; Tomasi, J.; Barone, V.; Cossi, M.; Cammi, R.; Mennucci, B.; Pomelli, C.; Adamo, C.; Clifford, S.; Ochterski, J.; Petersson, G. A.; Ayala, P. Y.; Cui, Q.; Morokuma, K.; Malick, D. K.; Rabuck, A. D.; Raghavachari, K.; Foresman, J. B.; Cioslowski, J.; Ortiz, J. V.; Baboul, A. G.; Stefanov, B. B.; Liu, G.; Liashenko, A.; Piskorz, P.; Komaromi, I.; Gomperts, R.; Martin, R. L.; Fox, D. J.; Keith, T.; Al-Laham, M. A.; Peng, C. Y.; Nanayakkara, A.; Gonzalez, C.; Challacombe, M.; Gill, P. M. W.; Johnson, B.; Chen, W.; Wong, M. W.; Andres, J. L.; Head-Gordon, M.; Replogle, E. S.; Pople, J. A. *GAUSSIAN 98 Rev. A.7 (G98W, V.5.2)*; Gaussian Inc.: Pittsburgh, PA, 1998.
(17) *Lange's Handbook of Chemistry*, 13th. ed.; Dean, J. E., Ed.; McGraw-Hill: New York, 1985.
(18) Bader, R. F. W. *op. cit.* See the discussion on pages 84 and 85.
(19) Kraulis, P. J. *J. Appl. Cryst.* **1991**, *24*, 946.